

Strathprints Institutional Repository

McKay, R.J. and Macdonald, M. and Bosquillon de Frescheville, Francois and Vasile, M. and McInnes, C.R. and Biggs, J.D. (2009) *Non-Keplerian orbits using low thrust, high ISP propulsion systems*. In: 60th International Astronautical Congress, 2009-10-12 - 2009-10-16, Daejeon, Korea.

Strathprints is designed to allow users to access the research output of the University of Strathclyde. Copyright © and Moral Rights for the papers on this site are retained by the individual authors and/or other copyright owners. You may not engage in further distribution of the material for any profitmaking activities or any commercial gain. You may freely distribute both the url (<http://strathprints.strath.ac.uk/>) and the content of this paper for research or study, educational, or not-for-profit purposes without prior permission or charge.

Any correspondence concerning this service should be sent to Strathprints administrator: <mailto:strathprints@strath.ac.uk>



McKay, R.J. and Macdonald, M. and Bosquillon de Frescheville, Francois and Vasile, M. and McInnes, C.R. and Biggs, J.D. (2009) Non-Keplerian orbits using low thrust, high ISP propulsion systems. In: 60th International Astronautical Congress, 12-16 October 2009, Daejeon, Korea.

<http://strathprints.strath.ac.uk/12919/>

This is an author produced version of a paper presented at the 60th International Astronautical Congress, 12-16 October 2009, Daejeon, Korea. This version has been peer-reviewed but does not include the final publisher proof corrections, published layout or pagination.

Strathprints is designed to allow users to access the research output of the University of Strathclyde. Copyright © and Moral Rights for the papers on this site are retained by the individual authors and/or other copyright owners. You may not engage in further distribution of the material for any profitmaking activities or any commercial gain. You may freely distribute both the url (<http://strathprints.strath.ac.uk>) and the content of this paper for research or study, educational, or not-for-profit purposes without prior permission or charge. You may freely distribute the url (<http://strathprints.strath.ac.uk>) of the Strathprints website.

Any correspondence concerning this service should be sent to The Strathprints Administrator: eprints@cis.strath.ac.uk

Non-Keplerian Orbits Using Low Thrust, High ISP Propulsion Systems

Robert McKay¹

robert.j.mckay@strath.ac.uk

Malcolm Macdonald¹

malcolm.mcdonald.102@strath.ac.uk

Francois Bosquillon de Frescheville²

Francois.Bosquillon.de.Frescheville@esa.int

Massimiliano Vasile³

m.vasile@aero.gla.ac.uk

Colin McInnes¹

colin.mcinnnes@strath.ac.uk

James Biggs¹

james.biggs@strath.ac.uk

¹Advanced Space Concepts Laboratory, University of Strathclyde, Glasgow, United Kingdom

²European Space Operations Centre, European Space Agency, Darmstadt, Germany

³Space Advanced Research Team, University of Glasgow, Glasgow, United Kingdom

ABSTRACT

The technology of high ISP propulsion systems with long lifetime and low thrust is improving, and opens up numerous possibilities for future missions. The use of continuous thrust can be applied in all directions including perpendicular to the flight direction to force the spacecraft out of a natural orbit (or A orbit) into a displaced orbit (a non-Keplerian or B orbit): such orbits could have a diverse range of potential applications. Using the equations of motion we generate a catalogue of these B orbits corresponding to displaced orbits about the Sun, Mercury, Venus, Earth, the Moon, Mars, Phobos and Deimos, the dwarf planet Ceres, and Saturn. For each system and a given thrust, contours both in and perpendicular to the plane of the ecliptic are produced in the rotating frame, in addition to an equithrust surface. Together these illustrate the possible domain of B orbits for low thrust values between 0 and 300mN. Further, the required thrust vector orientation for the B orbit is obtained and illustrated. The sub-category of solar sail enabled missions is also considered. Such a catalogue of B orbits enables an efficient method of identifying regions of possible displaced orbits for potential use in future missions.

FULL TEXT

I. INTRODUCTION

The concept of counter-acting gravity through a thrust vector was apparently first proposed by Dusek in 1966, who noted that a spacecraft could be held in an artificial equilibrium at a location some distance from a natural libration point if the difference in gravitation and centripetal force (gravity gradient) were compensated for by continuous low thrust propulsion [1]. More recently, this concept has been explored for the special case of solar sail propelled spacecraft which can, in principle, generate continuous thrust without the need for reaction mass [2]. The use of continuous thrust can

be applied in all directions including perpendicular to the flight direction, which forces the spacecraft out of a natural orbit (also known as an A orbit) into a displaced orbit (a non-Keplerian or B orbit): such orbits could have a diverse range of potential applications. Forward coined the term “statite” [3] in reference to a mission using a solar sail to hover above, or below, the Earth in such a displaced orbit in a concept which has become known as the Polar Observer, or PoleSitter, mission [4]. Following the work of Forward, McInnes made an extensive study of the concept [4], exploring new regions of interest, including the study of artificial, or displaced, Lagrange points which was considered

extensively in the late 1990's under the NASA/JPL/NOAA GeoStorm mission concept (which we discuss in more detail in Section V).

The work led by McInnes has since evolved to consider issues of orbit stability and control and has recently also considered other forms of propulsion including electric propulsion and the combination of SEP and solar sail technology [5]. Such work has focused primarily on Earth-centred trajectories, although many authors have considered individual applications of B orbits outwith the Earth's influence - for example, in-situ observation of Saturn's rings [6,7], or for lunar polar telecommunications [8]. As such, a systematic cataloguing of such opportunities throughout the solar system is of interest, to provide a platform for determining what missions may be enabled by low thrust, as opposed to suggesting a specific mission first and then deciding whether the spacecraft has sufficient thrust to achieve it.

II. DISPLACED NON-KEPLERIAN ORBITS

A. The Model

Following McInnes [7], the conditions for circular displaced non-Keplerian orbits can be investigated by considering the dynamics of a spacecraft of mass m in a reference frame $\mathbf{R}(x,y,z)$ rotating at constant angular velocity $\boldsymbol{\omega}$ relative to an inertial frame $\mathbf{I}(X,Y,Z)$. With such a system the equations of motion of the spacecraft are given by

$$\ddot{\mathbf{r}} + 2\boldsymbol{\omega} \times \dot{\mathbf{r}} + \nabla V = \mathbf{a} \quad (1)$$

where \mathbf{r} is the position vector of the spacecraft, dots denote differentiation with respect to time t , and V and \mathbf{a} are the augmented potential and the continuous and constant low thrust due to the propulsion system respectively, the former being given by

$$V = - \left[\left(\frac{1-\mu}{\|\mathbf{r}_1\|} + \frac{\mu}{\|\mathbf{r}_2\|} \right) \right] + \frac{1}{2} \|\boldsymbol{\omega} \times \mathbf{r}\|^2 \quad (2)$$

in units where the gravitational constant $G = 1$ and the system has total unit mass, and where μ is the reduced mass,

$$\mu = \frac{m_1}{m_1 + m_2} \quad (3)$$

and the latter being given by

$$\mathbf{a} = \left[\frac{T}{m} \right] \mathbf{n} \quad (4)$$

where \mathbf{n} is the direction of the thrust.

Setting $\ddot{\mathbf{r}} = \dot{\mathbf{r}} = 0$, i.e. assuming equilibrium conditions in the rotating frame, then the equation $\nabla V = -\mathbf{a}$

defines a surface of equilibrium points. Thus by specifying a range for the magnitude of \mathbf{a} the equation $\nabla V = -\mathbf{a}$ defines a series of nested surfaces of artificial equilibrium points, which can be plotted for a catalogue of planets in the Solar System.

Further, the required thrust vector orientation for an equilibrium solution is then given by,

$$\mathbf{n} = \frac{\nabla V}{\|\nabla V\|} \quad (5)$$

and the magnitude of the thrust vector, $\|\mathbf{a}\|$, is given by,

$$\|\mathbf{a}\| = \|\nabla V\|. \quad (6)$$

With these conditions the spacecraft is stationary in the rotating frame of reference. The only thing left to define then is the category used for the system in question: trajectories that make use of a continuous thrust-vector to offset gravity can be divided into two categories. The first category is the displacement of "traditional" orbits - for example, the displacement of the geostationary ring above the "traditional" ring which is within the equatorial plane. The second category of gravitationally displaced orbits is the displacement of Lagrange, or libration, points.

While the first category can be studied within the two-body problem the second requires the study of the three-body problem and can, with non-orientation constrained propulsion systems such as SEP, be equally applied to the Lagrange points of Planet-Sun systems as well as those of Moon-Planet systems. When considering orientation constrained propulsion systems, such as solar sailing, the displacement of Lagrange points in the Planet-Moon system becomes significantly more complex than for non-orientation constrained propulsion systems, as the Sun-line direction varies continuously in the rotating frame and the equations of motion of the sail are given by a set of nonlinear, non-autonomous ordinary differential equations: although one can analytically derive periodic orbits via a first-order approximation and use these in a numerical search to determine displaced periodic orbits in the full nonlinear model, such a study is beyond the scope of this paper. Thus our catalogue, whilst not limited in its consideration of solar electric propulsion, only considers the solar sail in the specific cases of the two-body system around the Sun and three-body systems where the sail is about a body that is itself orbiting the Sun.

B. The Three-Body Problem

The circular restricted three-body problem (CRTBP) provides a close approximation of the dynamics of a satellite operating in the vicinity of a planet within our

solar system, or a moon about its planet. Within the CRTBP the conditions for periodic circular displaced non-Keplerian orbits may be investigated by considering the dynamics of a spacecraft of mass m in a rotating frame of reference in which the primary masses m_1 and m_2 are fixed. In this system the x axis points between the primary masses, the y axis denotes the axis of rotation and the z axis is orthogonal to both. The position vector of the spacecraft in the CRTBP is thus given by $\mathbf{r} = (x, y, z)^T$ and the position vectors \mathbf{r}_1 and \mathbf{r}_2 of the spacecraft with respect to the primary bodies m_1 and m_2 are denoted by $\mathbf{r}_1 = (x + \mu, y, z)^T$ and $\mathbf{r}_2 = ((x - (1 - \mu)), y, z)^T$ respectively (see Figure 1), where μ is the reduced mass gravitational parameter that differentiates which body the spacecraft is in the vicinity of.

The equation for the magnitude of the thrust vector $\|\mathbf{a}\|$, as given above, then defines an implicit function in the x, y, z rotating coordinates. As an implicit function can be expressed in the form $f(x, y, z) = 0$ it defines a 3-D algebraic equithrust surface which can be conveniently plotted.

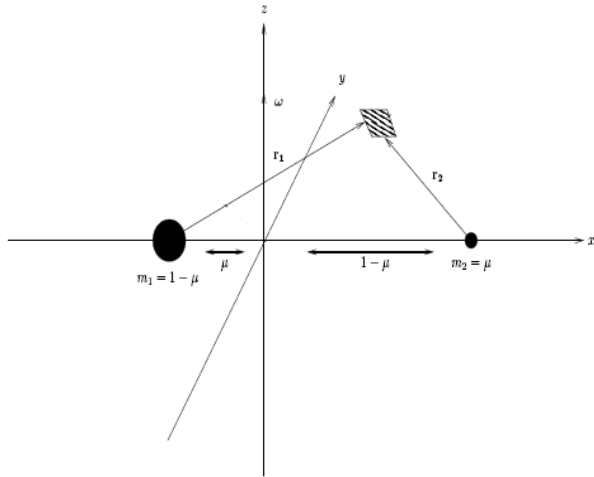


Fig. 1: The rotating coordinate frame and the spacecraft position therein for the restricted three-body problem

In the case of the solar sail, acceleration is constrained by its lightness number,

$$\mathbf{a} = \beta \frac{1 - \mu}{r_1^2} (\hat{\mathbf{r}}_1 \cdot \mathbf{n})^2 \mathbf{n} \quad (7)$$

where β is the sail lightness number (the ratio of the solar radiation pressure force to the solar gravitational force exerted on the sail), and its orientation – naturally, a solar sail cannot have a component of thrust towards the Sun, and thus there are regions in which a solar sail cannot execute B orbits. Equation 5 on its own only determines the thrust contours assuming that the spacecraft could thrust in that direction if desired - thus

one must determine the orientation of the thrust vector and automatically specify a thrust of zero if the thrust vector has any component directed towards the Sun.

C. The Two-Body Problem

The two-body problem is simply the limiting case of the three-body problem where the secondary mass $m_2 = 0$.

However, note that, whilst SEP spacecraft are considered for various bodies in the Solar System, as the orientation-constrained nature of the solar sail propulsion is significantly more complex (and thus beyond the scope of this study) we only consider solutions for a solar sail that is orbiting the Sun (in the 2-body case) or about a body that is orbiting the Sun (in the three-body case).

Without the complication of a second mass (and therefore a third dimension to the problem), it is simpler just to use a set of cylindrical polar coordinates (ρ, z) rotating with constant angular velocity $\boldsymbol{\omega} = \omega \hat{\mathbf{z}}$, relative to an inertial frame I as shown in Figure 2.

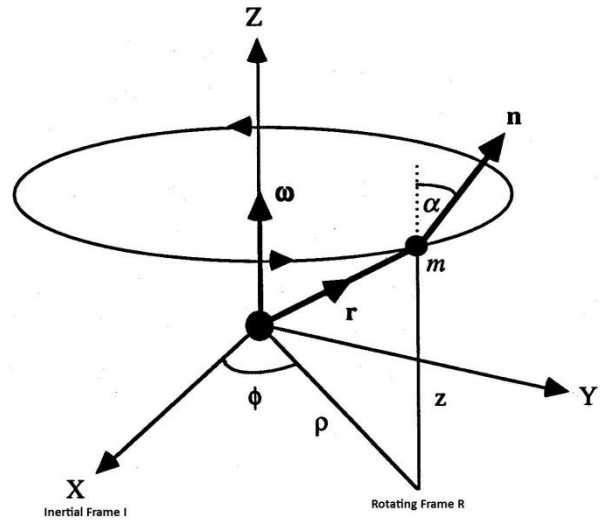


Fig. 2: Two-body displaced non-Keplerian orbit of spacecraft with thrust-induced acceleration

The augmented potential in the rotating frame can then be written as

$$V(\rho, z; \omega) = - \left[\frac{1}{2} (\rho \omega)^2 + \frac{GM}{r} \right] \quad (8)$$

where we have moved back into SI units. Since ω is constant, there can be no transverse component of thrust, so the thrust vector is pitched in the plane spanned by the radius vector and the vertical axis and is thus defined by a single pitch angle α , which is given by

$$\tan \alpha = \frac{\|\hat{\mathbf{z}} \times \nabla V\|}{\hat{\mathbf{z}} \cdot \nabla V} = \left(\frac{\rho}{z}\right) \left[1 - \left(\frac{\omega}{\omega_*}\right)^2\right]^2 \quad (9)$$

where

$$\omega_*^2 = \frac{GM}{r^3} \quad (10)$$

The thrust-induced acceleration is thus given by

$$a(\rho, z; \omega) = [\rho^2(\omega^2 - \omega_*^2)^2 + z^2\omega_*^4]^{1/2} \quad (11)$$

Since the spacecraft is stationary in the rotating frame of reference, in an inertial reference frame the spacecraft appears to execute a circular orbit displaced above the central body, as illustrated in Figure 2.

The addition of the thrust-induced acceleration generates 3 types, or families, of circular non-Keplerian orbits that have their centre displaced above the central body, parameterised by the spacecraft orbit period (note that the orbital period was not a parameter of the three-body case due to the necessity of the spacecraft to orbit the primary mass at the same orbital velocity of the secondary body). The three types of orbit are characterised as:

- Type I: orbit period fixed for given r
- Type II: orbit period fixed for given ρ
- Type III: all displaced orbits have same orbital period as a selected reference Keplerian orbit.

D. Type I Orbits

Type I orbits are seen when the required thrust-induced acceleration is at its global minimum, which occurs when the orbit period is chosen such that $\omega = \omega_*$. Hence the thrust-induced acceleration and required pitch angle reduce to

$$a = \frac{GMz}{r^3} \quad (12)$$

and

$$\tan \alpha = 0 \quad (13)$$

respectively, with the acceleration simply being a function of ρ and z .

E. Type II Orbits

Type II orbits are generated by selecting

$$\omega = \sqrt{GM/\rho^3} \quad (14)$$

i.e. where the spacecraft is synchronous with a body on a circular Keplerian orbit in the $z = 0$ plane with orbit

radius ρ . The acceleration and thrust direction equations are then given by

$$a = \left(\frac{GM}{r^2}\right) \left[1 + \left[1 + \left(\frac{z}{\rho}\right)^2\right]^2 \left[1 - 2 \left[1 + \left(\frac{z}{\rho}\right)^2\right]^{-3/2}\right]\right]^{1/2} \quad (15)$$

and

$$\tan \alpha = \left(\frac{\rho}{z}\right) \left[1 - \left[1 + \left(\frac{z}{\rho}\right)^2\right]^{3/2}\right]. \quad (16)$$

F. Type III Orbits

A third family of two-body orbits exists where the orbital period of the spacecraft is fixed to be constant throughout the $\rho - z$ plane, i.e. $\omega = \omega_0$, and thus the acceleration and thrust direction equations become

$$a = [\rho^2(\omega_0^2 - \omega_*^2)^2 + z^2\omega_*^4]^{1/2} \quad (17)$$

and

$$\tan \alpha = \left(\frac{\rho}{z}\right) \left[1 - \left(\frac{\omega_0}{\omega_*}\right)^2\right] \quad (18)$$

respectively. Then a value of $\omega = \omega_0$ can be chosen such that the displaced orbits are synchronous with a Keplerian orbit with either a specific orbital radius ρ , or a specific orbital period P , remembering that

$$\left(\frac{P}{2\pi}\right)^2 = \frac{r^3}{GM} = \frac{1}{\omega_*^2}. \quad (19)$$

This results in two distinct branches of solutions corresponding to orbits in the $z = 0$ plane or orbits displaced above this plane.

III. NON-KEPLERIAN ORBIT CATALOGUE

Essentially, the family of non-Keplerian displaced B orbits can be summed up very simply in a single diagram, as shown in Figure 3.

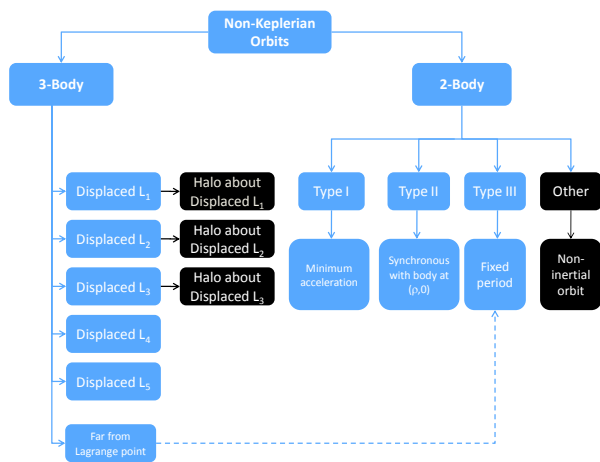


Fig. 3: Summary of possible non-Keplerian orbits

The primary distinguishing feature of the catalogue is the gravitational potential well of the system, information which is encoded in the parameter μ . The two-body problem is a limiting case of the three-body problem with $m_2 = 0$, however, the two-body problem gains an extra free parameter - as discussed previously, several families of two-body orbits exist, parameterised by the choice of the orbital period. This choice does not exist in the three-body model due to the requirement the orbital period of the spacecraft be fixed to that of the secondary body as it orbits the primary. Thus different types of orbit exist for the two-body case, with different characteristics, as shown in Figure 3. The black box for “Other” indicates fundamentally different types of two-body non-Keplerian orbit – for example, non-inertial orbits, which involve precession or rotation of, say, the ascending node angle - and as such are not covered within this activity. However, it is worth pointing out that there are several examples of such orbits having been considered within the literature – such as, for example, the GeoSail concept considered by Macdonald and co-workers [9], or the Sun-synchronous orbit around Mercury discussed by Leipold et al. [10,11].

In the three-body case one can have B orbits displaced around any of the Lagrange points, although generally the regions in the vicinity of the L_1 and L_2 points are where the most spatial variation of the equithrust contours/surfaces occurs in the three-body case. It is also possible to generate halo orbits around the displaced L_1 , L_2 and L_3 points, but we do not consider those here and thus they are also represented by black boxes. As one moves far away from the second body in a three-body problem, the contours for the two- and three-body problem become identical (with the aforementioned proviso that the orbit period is always fixed to that of the secondary body), hence the dashed line in Figure 3 representing the reduction of the three-body problem to the two-body problem far away from the secondary body.

The amount of thrust available to the spacecraft will determine the exact size/range of the contours that are accessible. We consider a thruster with a maximum thrust of 300mN and a specific impulse of 4500 seconds, in order to consider mission opportunities with currently available or near-term technology such as the QinetiQ T6 thruster, which will provide a thrust up to 230mN at a specific impulse of above 4500 seconds for the BepiColombo mission [12]. The contour plots are then essentially independent of the bodies involved, other than the actual size of the contours accessible due to the differing gravitational potential wells.

The only other complexity that exists is then related to the actual propulsion system used – i.e. SEP (solar electric propulsion) or solar sail - however, once again, the basic contour topology remains independent of the bodies being considered. As such when we consider actual mission opportunities to exploit B orbits, every orbit can be categorised as per Figure 3.

Thus a catalogue of B orbits and their associated required thrust directions for specific bodies in the solar system can be identified for both the two-body and three-body orbit cases as defined above – some examples of these plots are illustrated below. The specific bodies investigated for the catalogue are listed below:

- Sun
- Mercury
- Venus
- Earth
 - the Moon
- Mars
 - Phobos
 - Deimos
- Ceres
- Saturn

although in principle any planet, asteroid or celestial body could be considered – however, of course, providing enough photon flux/momentum to power the SEP/sail respectively would naturally have to be taken into consideration.

A catalogue of such B orbits will enable a quick and efficient method of identifying regions of possible displaced orbits for potential use in future missions. A selection of examples taken from the catalogue are presented in Section IV below, and a more detailed discussion of two potential missions utilizing non-Keplerian orbits is discussed in Section V.

IV. ORBIT CATALOGUE EXAMPLES

Primarily to indicate how the various types of orbit appear in practice, in this Section we include some examples for the case of displaced orbits about Mars for both the two-body and three-body cases as outlined above – as discussed previously, the thrust contours for different bodies are not fundamentally different other than the physical extent of them.

A. Two-body

Figure 4 displays the Type I orbits in the vicinity of Mars. In this plot the dashed lines represent contours of constant period, the coloured contours represent the thrust contours and as such are labeled with the value of the thrust (in milli-Newtons) and the arrows represent the thrust direction required to maintain such an orbit.

The thick black contour of radius 170 planetary radii represents the sphere of influence boundary of Mars, calculated via the equation

$$r_{SOI} = a_p \left(\frac{m_p}{m_s} \right)^{2/5}, \quad (20)$$

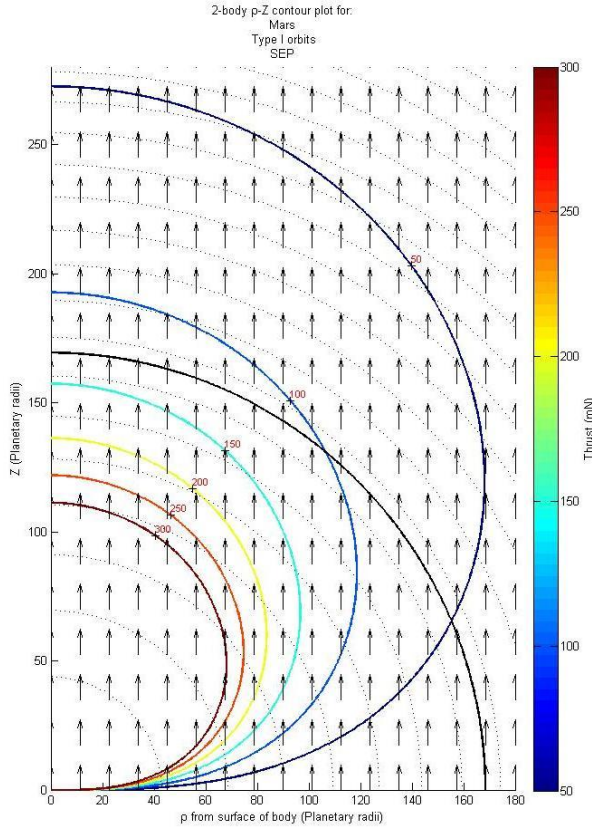


Fig. 4: Two-body Type I orbits for Mars – the coloured lines represent the thrust contours (labelled in mN), the arrows represent the thrust direction, the dashed lines represent contours of constant orbital period and the black line represents the sphere of influence boundary of Mars.

where a_p is the semi-major axis of the planet’s orbit in relation to the largest body of the system - in this case, the Sun – and m_p and m_s are the masses of the planet and Sun respectively (of course, if one were studying, say, Phobos, then we would consider the orbital distance of the moon from its parent Mars to obtain the sphere of influence). Beyond this boundary technically the validity of the two-body model comes increasingly under question as the gravitational attraction of the third body (i.e. the Sun) approaches the same influence as that of the body being studied (i.e. Mars), and at this point one should at least be starting to consider the three-body model. However, thrust contours that extend beyond this boundary are not automatically invalidated, rather just increasingly perturbed, and thus it is still instructive to show them on our plots.

We can see that with such an orbit we can hover directly above the planet, which is the “statite” orbit as termed by Forward. The greater the amount of thrust available to the spacecraft, the greater the gravity gradient it can compensate for and thus the closer the hover to the planet. The Type I orbits are designed to maximize the distance from the body for the minimum thrust, hence the rather elongated nature of the contours.

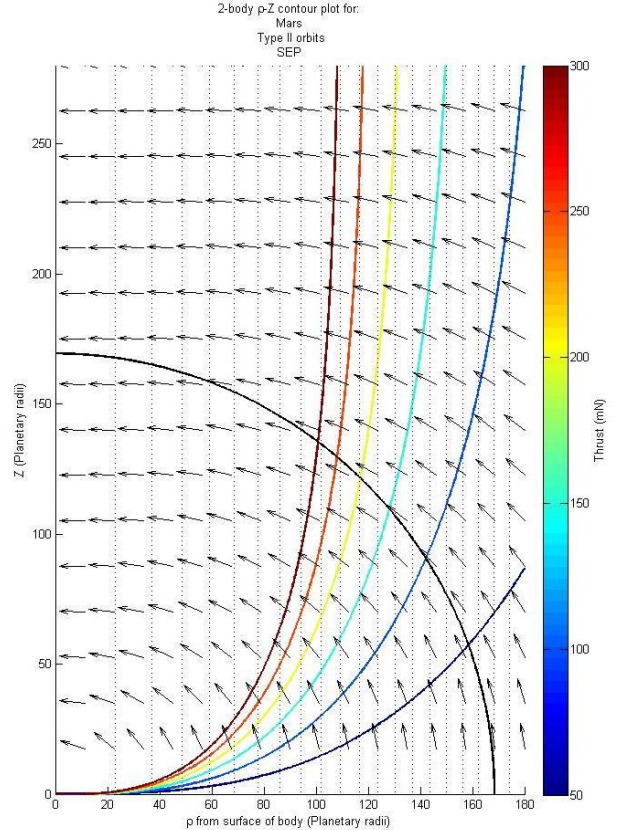


Fig. 5: Two-body Type II orbits for Mars, with the thrust direction, orbit period contours and sphere of influence depicted in the same way as Fig. 4.

Figure 5 shows the Type II orbits for Mars. These orbits are synchronous with a Keplerian orbit in the $z = 0$ plane with orbit radius ρ . These orbits are only achieved with a component of thrust directed towards the body, so a solar sail could not execute a Type II orbit about the Sun.

The Type III orbit plots are dependent on which point in the $z = 0$ plane the spacecraft orbit is synchronous with. Figure 6 shows the equithrust contours for a value of ω_0 chosen such that the displaced orbits are synchronous with a Keplerian orbit with radius $\rho = 110$ Mars radii. We can see, as stated previously, the two distinct branches of solutions corresponding to orbits in the $z = 0$ plane or orbits displaced above this plane. Equivalently rather than specify a point to be synchronous with one can specify an orbital period, since the two are linked via Kepler's laws.

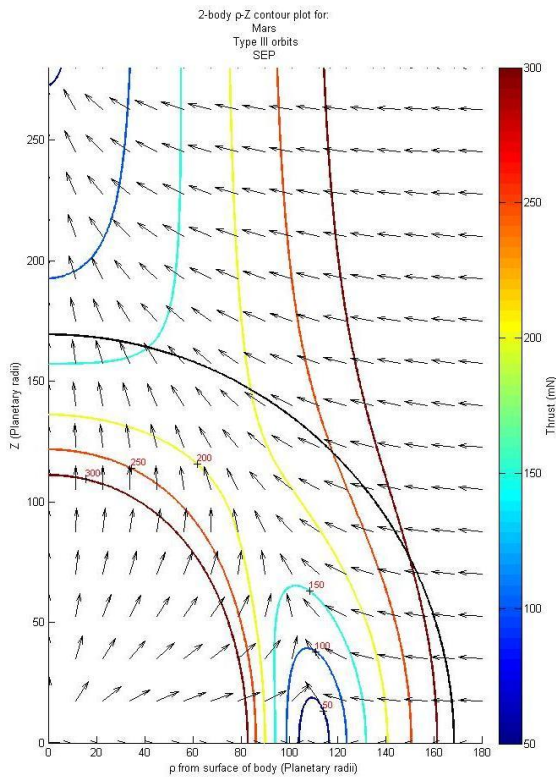


Fig. 6: Two-body Type III orbits for Mars, synchronised with a Keplerian orbit with radius $\rho = 110$ Mars radii.

One can also note validation between the different orbit types – for example, in the regions in Figure 6 where the thrust direction is oriented directly upwards (i.e. $\alpha = 0$), the spacecraft is displaced the same height above the body, as one would expect.

B. Three-body

Staying with Mars, we can consider the case when the influence of the Sun is taken into account, i.e. the three-body Sun-Mars case. Figure 7 shows the B orbit regions about Mars projected onto a plane parallel to

the ecliptic plane, and the thrust direction required to enable the orbit.

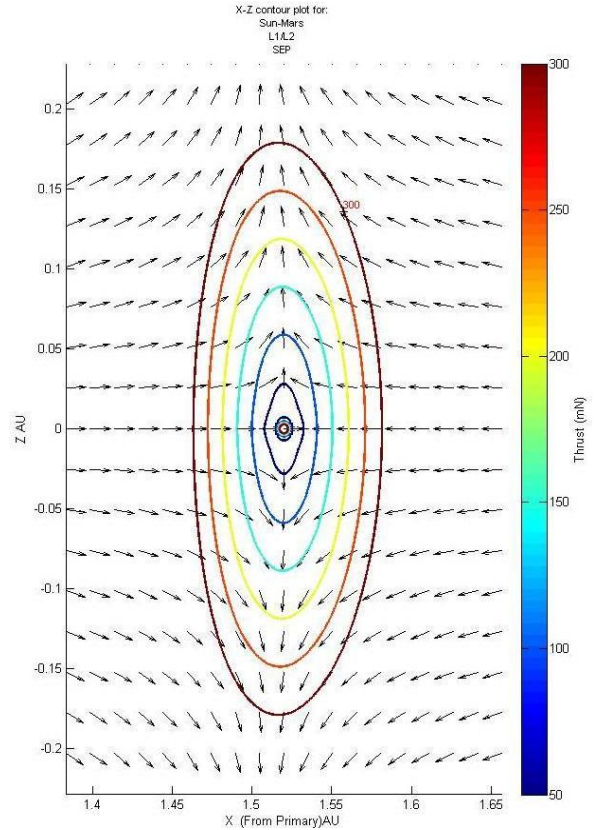


Fig. 7: B orbit zones depicted by equithrust contours for the Sun-Mars three-body case, projected onto the plane perpendicular to the Ecliptic plane. The required thrust direction is indicated by the arrows.

As was stated previously, we see that far away from the body the contours resort to that of the two-body case. One can imagine utilising such orbits to hover directly above or below Mars at significant distances (indeed, we discuss the potential applications for such orbits in the next section), or alternatively one could station a craft in the Mars orbital plane up to 0.06au closer to or further from the Sun, and still maintain the same orbital period as the planet.

We can consider the same scenario for a solar sail instead of a solar electric propulsion spacecraft. For a direct comparison, we do not consider the solar sail in terms of sail beta but simply assume the sail has the same thrust-to-mass ratio for a smaller spacecraft mass, i.e. consider a maximum thrust of 30mN for a 100kg solar sail spacecraft. Figure 8 shows the thrust contours for the case of orbits projected onto a plane parallel to the ecliptic plane, for the same scale as the solar electric propulsion case as in Figure 7. We can see that the B orbit region for the sail is considerably smaller as the direction of thrust is fixed by the direction of photon flux from the Sun, and hence there is a smaller component of thrust in the direction required to achieve a non-Keplerian orbit - unlike the SEP spacecraft,

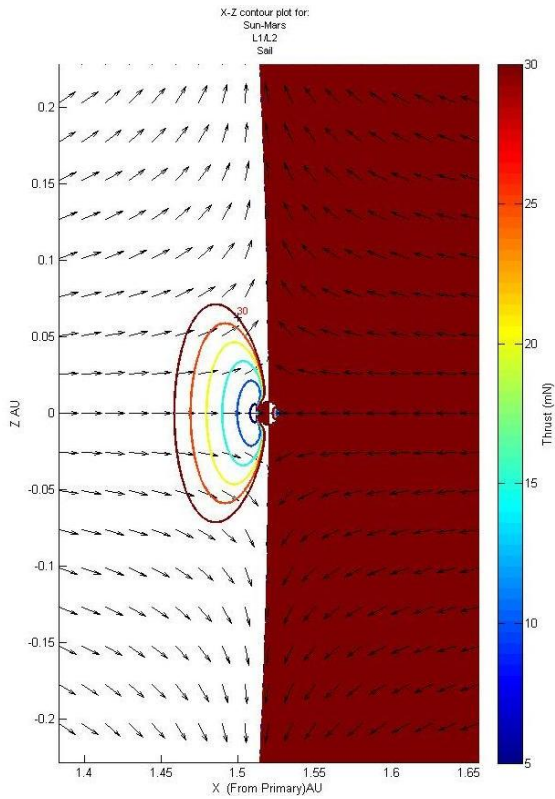


Fig. 8: B orbit zones depicted by equithrust contours for the Sun-Mars three-body, case projected onto the plane perpendicular to the Ecliptic plane, for a solar sail. The same scale as in Fig. 8 is used. The filled regions represent forbidden zones for the solar sail.

which can be oriented to have the maximum component of thrust in the required direction.

The filled region in Figure 8 represents a forbidden region for the solar sail, where the spacecraft would have to have some component of thrust towards the Sun, which is not possible: thus there are areas which are accessible to an electric propulsion system that are not necessarily accessible to a sail.

Figure 9 shows a zoomed-in version of Figure 8, to show the solar sail's displaced orbits around both Lagrange points L_1 and L_2 , although the region around L_2 where B orbits are possible is considerably smaller than that of L_1 due to the required thrust direction in this region being directed away from the $z = 0$ plane, unlike around L_1 where the arrows are much closer to being parallel to this plane.

The Mars case is quite different to many of the other cases we consider in our catalogue. The gravitational potential well at Mars is much shallower than that of, say, Mercury, and so the thrust contours about L_1 and L_2 of Mercury look quite different because 300mN is not nearly enough to be far away so as to effectively reduce the problem to a two-body one, as shown in

Figures 10 and 11 (of course, given sufficient thrust, we would see that same shape contours for both cases).

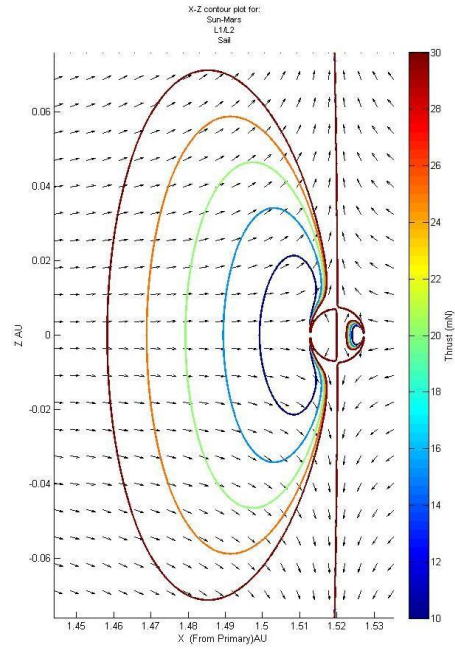


Fig. 9: A zoomed-in version of Fig. 8, showing B orbit zones depicted by equithrust contours projected onto the plane perpendicular to the Ecliptic plane for the Sun-Mars three-body case for a solar sail.

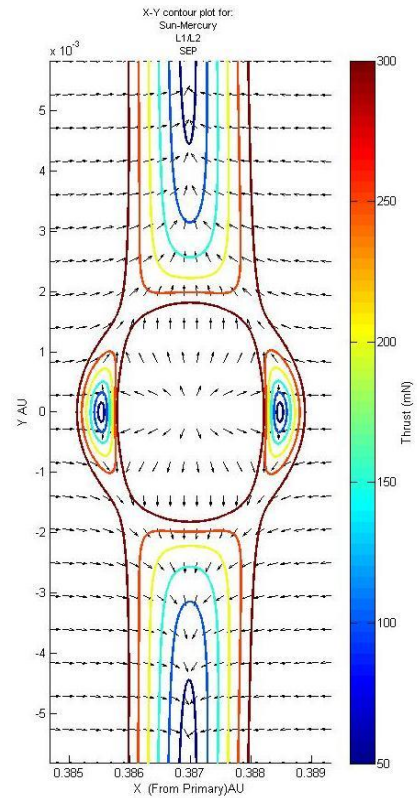


Fig. 10: B orbit zones depicted by equithrust contours projected onto the plane parallel to the Ecliptic plane, for the Sun-Mercury three-body case, for a SEP spacecraft.

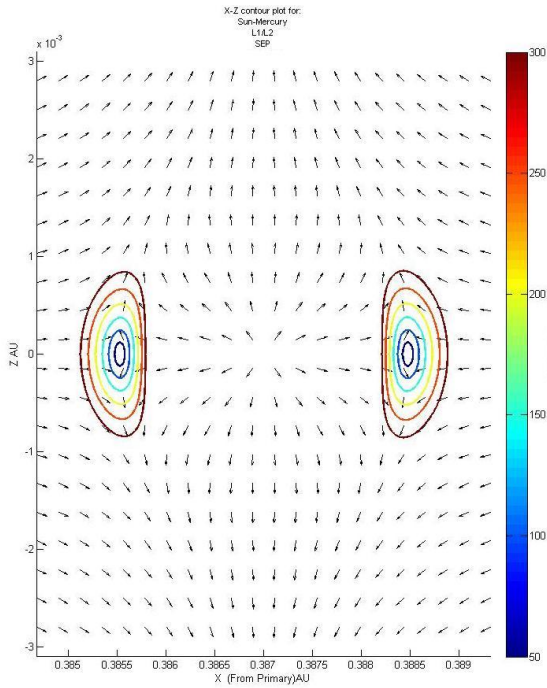


Fig. 11: B orbit zones depicted by equithrust contours, projected onto the plane perpendicular to the Ecliptic plane, for the Sun-Mercury case for a SEP spacecraft.

We can also produce three-dimensional equithrust surfaces in order to aid our understanding of the region B orbit zones exist for around a given body. Figure 12 shows the 300mN equithrust surface around the Mercury L1 and L2 points for SEP thrust, illustrating the location of Mercury in relation to the surface as well as showing the direction of the Sun and Mercury's orbit.

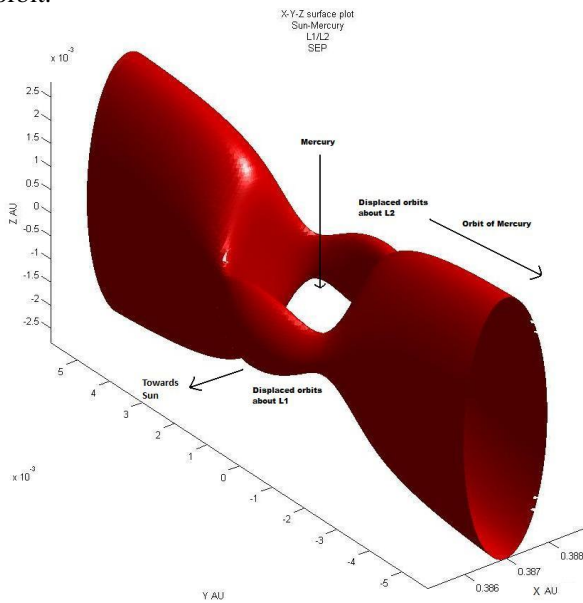


Fig. 12: 300mN equithrust surface for the Sun-Mercury L_1/L_2 system.

We can see that, unlike the Mars case, we do not have sufficient thrust to hover directly above Mercury in this

case, but we can displace a spacecraft to a B orbit round Mercury in the ecliptic plane, and to a variety of different points above the ecliptic plane.

One might then think of hovering directly above Mercury by considering the 2-body Type I case for such an orbit instead. However, although our two-body model suggests a thrust of 300mN would allow a spacecraft to hover approximately 1.8×10^{-3} AU directly above Mercury using such an orbit, this would be outside the sphere of influence boundary of Mercury as given by Eq. (20) and thus would require a full three-body treatment to be considered valid – which, as indicated above by Fig. 12, suggests that the addition of the third body limits the regions the spacecraft could occupy with 300mN and thus rules out hovering directly above Mercury.

V. CANDIDATE MISSION OPPORTUNITIES

Such B orbits could have a diverse range of potential applications for Earth observation, space physics, human exploration and planetary science. In this section, we discuss two possible candidates chosen from the B orbit catalogue, outlining the science case, how it would be achieved, and estimating on-station mission durations. It is anticipated that more detailed analysis will be carried out on these examples in the future, to include more detailed delta-v budgets, insertion trajectories and mission timelines, as well as including propulsion failure scenarios.

A. GeoStorm

Magnetic storms pose a high risk to electrical and telecommunications equipment at both the Earth's surface and in the lower atmosphere. It is believed that such bombardments of high-energy particles are caused by solar coronal mass ejections (CME's). The concept for the GeoStorm mission originated in the late 1990's after the National Oceanic and Atmospheric Administration (NOAA) asked the Jet Propulsion Laboratory (JPL) if it was possible to improve the warning time of such an impending space weather event via the application of emerging new technologies such as solar sails and micro-spacecraft. Probes orbiting the Earth-Sun L_1 point can provide approximately 30 minutes advance warning of an approaching CME. The aim of the resulting 1999 ST-5 GeoStorm proposal mission was to use a solar sail of characteristic acceleration 0.169mms^{-2} to access an artificial displaced orbit at a point sunward of L_1 (0.993AU from the Sun), instead maintaining station at 0.984AU [13]. This would increase the warning time of an approaching magnetic storm by a factor of approximately 3.

A nominal trajectory for GeoStorm involved a transfer time of 3 months from LEO to L_1 on a ballistic trajectory and then a sail trajectory of 192 days to move

from L_1 to sub- L_1 [14]. The ST-5 design was not chosen by NASA for flight demonstration; however, it did highlight the performance potential. Further work by JPL [13] involved an improved solar sail design that would allow a craft of mass approximately 95kg and characteristic acceleration 0.438mms^{-2} , to maintain station at 0.974AU, increasing the warning time yet further (by another factor of 2 compared to the 1999 mission proposal).

We can apply the same principle to a continuous low-thrust SEP spacecraft of mass 1000kg, and, from our orbit catalogue, consider the displaced orbits around Earth's L_1 point by studying the Sun-Earth three-body system. Figure 13 shows displaced orbit locations in the x, z plane through $y = 0$ (i.e. so that the spacecraft is on the Earth-Sun line, orbiting the Sun with the same period as the Earth).

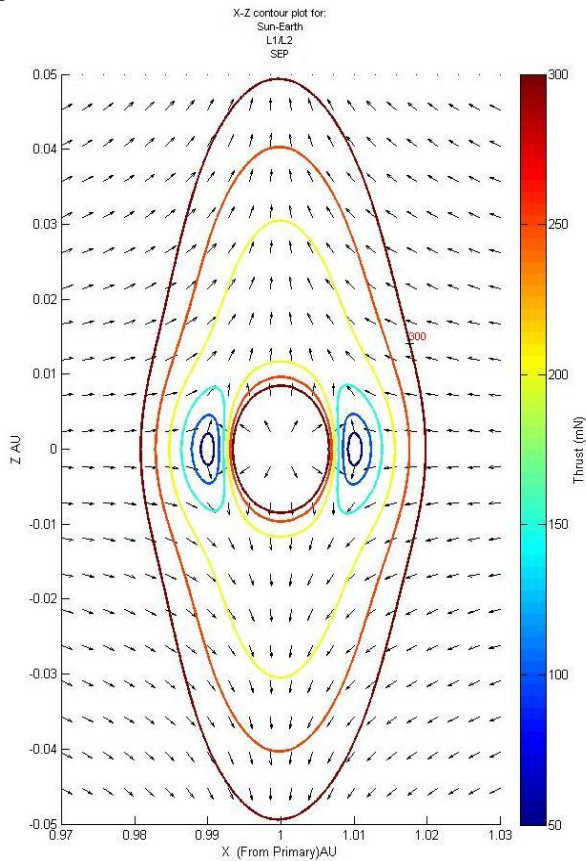


Fig. 13: B orbit zones depicted by equithrust contours, projected onto the plane perpendicular to the Ecliptic plane for the Earth-Sun L_1/L_2 system corresponding to thrust values of 50mN, up to a maximum of 300mN (labelled). The arrows indicate the required thrust direction.

We can see that, although an orbit at 0.974AU would not be achievable due to the high mass of the craft, 300mN of thrust would make it possible to station at approximately 0.9807AU from the Sun. At such a point the thrust direction arrows indicate the spacecraft would

need to thrust radially away from the Sun along the Earth-Sun line to maintain such a position.

This would allow for a geomagnetic storm warning time of upwards of 90 minutes. Of course the finite amount of propellant stored on board the SEP spacecraft clearly means that this position could only be maintained for a finite time. We can estimate this on-station duration as follows: assuming our SEP spacecraft has a thruster which has a maximum thrust of 300mN and a specific impulse of 4500sec, and the spacecraft is of total mass 1000kg, 500kg of which is propellant, then the total Δv of the spacecraft can then be calculated from the rocket equation

$$\Delta v = I_{SP} g_0 \ln \left(\frac{m_0}{m_1} \right) \quad (21)$$

where I_{SP} is the specific impulse of the thruster, g_0 is the gravitational acceleration at sea level, m_0 is the initial total mass, including propellant and m_1 is the final total mass. The estimated Δv to achieve orbit insertion is then subtracted from this, indicating how much delta-v is available for thrusting on station. Then the on-station duration Δt is simply

$$\Delta t = \frac{\Delta v}{a} \quad (22)$$

where a is the acceleration of the spacecraft due to continuous thrust. Thus assuming that the spacecraft has already been launched to LEO, to get to the position (0.9807AU from the Sun or alternately 0.0193AU from the Earth) requires a delta-v of approximately 4kms^{-1} , and the previous two equations combined give an on-station duration at maximum thrust of approximately 3 years. This would thus necessitate future missions to re-establish a warning post. In theory a solar sail could remain on-station for an infinite amount of time, although in practice degradation of the reflective surface and on-board electronics would eventually terminate the mission.

It may also be of interest to note that a spacecraft capable of producing 1000mN could be displaced as far as 0.05AU from Earth, i.e. 0.95AU from the Sun, which would increase warning times still further by a significant amount. Clearly, though, such thrust capabilities are not yet on the horizon in terms of technical feasibility.

B. Mars-Earth Communication Relay

For the exploration of Mars, continuous communication is required. Currently, during periods of solar occultation assets both in-orbits about Mars and on its surface are out of communication with ground

controllers. While such a scenario is acceptable for robotic assets it is not for human exploration, and as such a communication relay is required to ensure continuous communication between Earth and Mars. It is noted that any spacecraft within the Ecliptic plane (or even which passes through the Ecliptic plane) shall experience periods of solar occultation of Earth, as such, we must consider non-Keplerian orbits outwith the Ecliptic plane.

Figure 14 illustrates the architecture options of a Mars-Earth communication relay, assuming a four-degree field-of-view exclusion zone about the Sun as viewed from Earth.

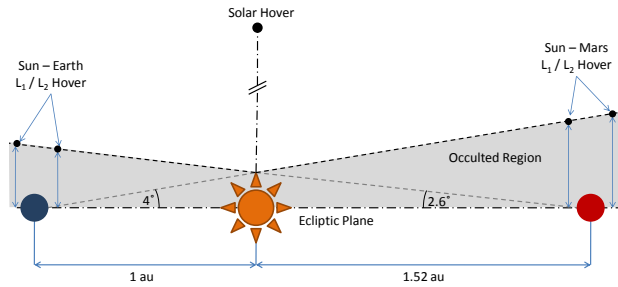


Fig. 14: Mars – Earth communication relay architecture options out of the Ecliptic plane (not to scale).

Note that although points above the Ecliptic plane are illustrated the architecture is symmetrical about the Ecliptic plane. For design optimisation of the communication system, a spacecraft in proximity of Mars is preferred as the long slant range back to Earth can be compensated for through the use of a large Earth based antenna. From Figure 14, note further that hover points above L_2 are slightly further from the Ecliptic plane, and thus it will require a slight amount of extra thrust to maintain these points.

The Sun – Mars stations can be determined to be located approximately 0.176AU out of the Ecliptic plane (as stated above, assuming a 4-degree field-of-view exclusion from Earth), while the Sun – Earth stations can be determined to be located approximately 0.116AU outwith the Ecliptic plane (if the equivalent spacecraft-Mars-Sun angle is taken to be 2.64°). As discussed in the previous section, the much shallower gravitational potential well at Mars significantly increases the distance from the planet that a spacecraft can hover at in comparison to Earth.

It is therefore of great interest to note that the value of 0.176AU for a Mars station is just within the range achievable by a continuous low-thrust spacecraft of 300mN, as illustrated in Figure 15, making a Mars hover a particularly strong candidate for further study. (Note that Figure 15 is essentially just the same as Figure 7, but with additional intermediate contours.)

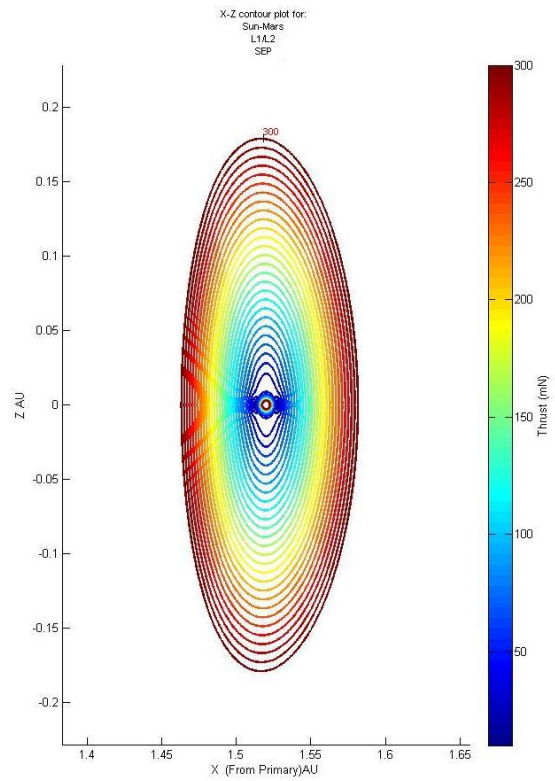


Fig. 15: B orbit zones depicted by equithrust contours projected onto the plane perpendicular to the Ecliptic plane for the Mars-Sun three-body system, for SEP of thrust values of up to 300mN with contours each representing 10mN.

An interesting extension to this concept is to consider spacecraft in displaced orbits either leading or trailing the orbit of Mars, i.e. in the Ecliptic plane. Considering the symmetry of Figure 14, the 4-degree field-of-view exclusion defines a conic region around the Sun where Mars is hidden from the Earth. If we consider this conic region end-on from behind Mars, as shown in Figure 16, we can consider that, as well as achieving continuous communications by displacing a spacecraft directly above Mars, one could also displace a spacecraft onto the circular (when projected in two dimensions) region around Mars defined by the field-of-view exclusion, so that one spacecraft was trailing and the other leading the orbit of Mars.

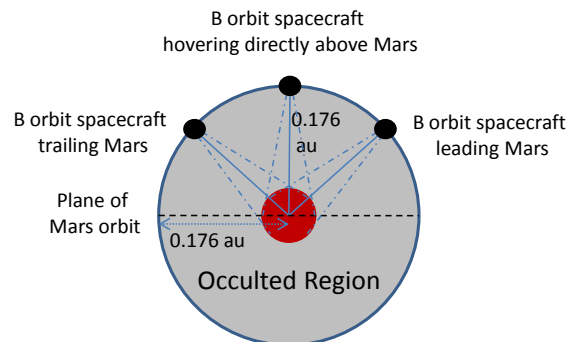


Fig. 16: End-on view of the Mars–Earth communication relay architecture options, looking along the Ecliptic plane.

Naturally, as they track Mars they too will enter the blackout region: as depicted in Figure 16, the leading spacecraft will move beyond the edge of the blackout region as the trailing spacecraft moves into this region. However, the separation of the two spacecraft means that only one will ever be in this region at any given time, and, hence, provided the spacecraft are displaced far enough above the plane of the orbit of Mars to maintain a line-of-sight between themselves, as illustrated in Figure 16, then continual communications can still be achieved by relaying the signal from the occulted spacecraft to the one outside the occulted region and then on to Earth.

There are other advantages to considering this dual spacecraft option over the case of a single spacecraft hover. Firstly, hovering directly above Mars limits communications to just the polar regions. If the spacecraft are trailing/leading the orbit then communication with the equatorial regions is enabled. A second advantage can be shown by considering the thrust contours in the plane illustrated by Figure 16, i.e. the y - z plane, as shown in Figure 17.

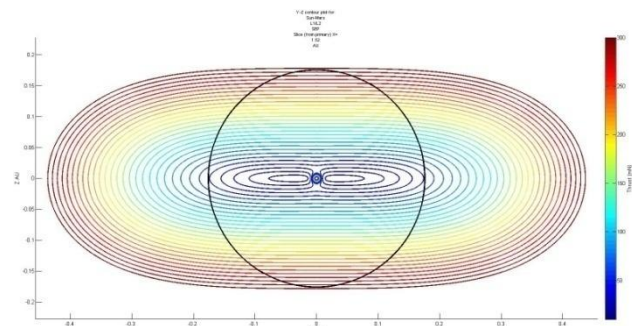


Fig. 17: An end-on view of B orbit zones depicted by equithrust contours of up to 300mN about Mars, looking along the Ecliptic plane. The black circle represents the extent of the occulted region.

As can be seen it is easier to displace the spacecraft orbit from Mars in this plane than out of it and so a spacecraft can occupy a B orbit region on the surface defined by the field-of-view exclusion for less thrust if it trails or leads Mars rather than hovering directly above. So, practically, it may be more feasible to maintain the communications relay using two spacecraft with lower thrust than a single spacecraft which needs higher thrust.

Technically the circular orbit of Mars and the spacecraft means that the arc drawn out as they pass through the occulted region is not confined to a single slice in the y - z plane, but as the arc length is relatively small compared to the diameter of the orbit it is reasonable to approximate the arc to a straight line (and thus the spherical surface, defined by the arc, to a Cartesian plane) to illustrate the point. A more detailed analysis

of the contours would require projecting contours onto this spherical surface.

Further, one could potentially induce a non-Keplerian orbit to displace the spacecraft in either (leading or trailing) orbit closer to or further from the Earth (see Figure 18).

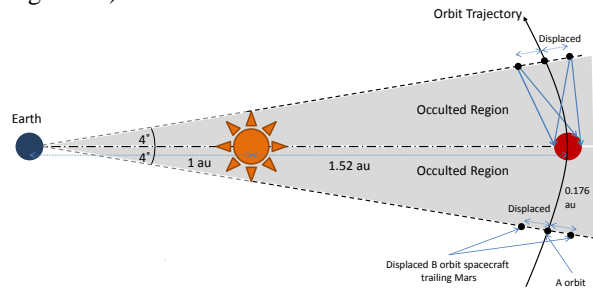


Fig. 18: Mars – Earth communication relay architecture options in the Ecliptic plane (not to scale).

We can see that a maximum thrust of 300mN allows a spacecraft to be displaced up to a maximum of approximately 0.06AU closer to (or further from) the Earth, as shown in both Figures 15 and 19, and still maintain an orbit with the same orbital velocity as that of Mars, allowing it to track the planet at a constant distance.

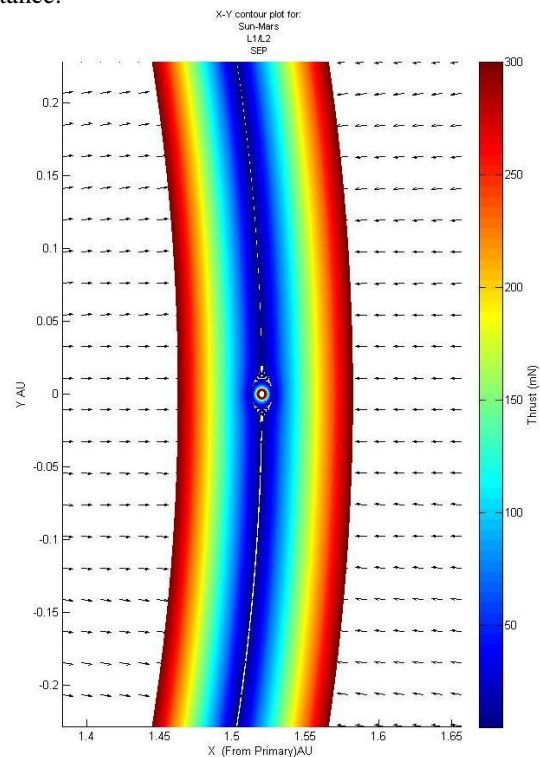


Fig. 19: B orbit zones depicted by equithrust contours, projected onto the plane parallel to the Ecliptic plane for the Mars-Sun three-body system in the Ecliptic plane, for SEP of thrust values of up to 300mN.

This displacement is of course dependent on the plane of the orbit, so displacing higher above Mars makes it harder to displace closer to Earth. Such a position will be considered in a detailed mission study because there is clearly some trade-off to be made between communicating with a specific region on the surface, maintaining an optimal line-of-sight between the two spacecraft, minimising the signal travel time between the spacecraft and the Earth and doing all this for the minimum amount of thrust. As an example, consider the case where, rather than having both spacecraft above the plane of the orbit Mars one is instead below this plane, as in Figure 20:

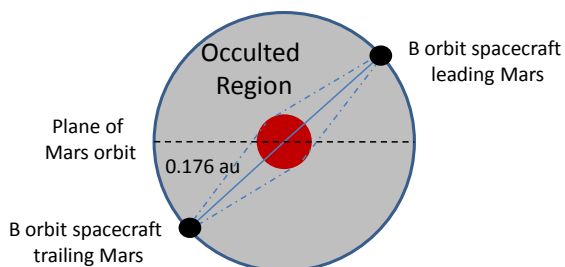


Fig. 20: End-on view of an alternative Mars – Earth communication relay architecture option, looking along the Ecliptic plane.

This configuration would require two spacecraft with the same thrust as the configuration in Figure 16, but with the added advantage of covering most of both hemispheres of Mars, unlike the configuration in Figure 16. Given the distance between the spacecraft, the arc of the orbit should be sufficient to maintain the line-of-sight (i.e. one will not be occulted by Mars with respect to the other) - but if not one could of course displace them far enough from the planet in the plane of the orbit of Mars (i.e. towards/away from Earth, as depicted in Figure 18) to ensure that the line-of-sight is restored, although this would require more thrust as we would be displacing away from Mars in two planes, not just one.

Figures 21 and 22 illustrate a possible insertion trajectory to the point 0.176AU above Mars. This trajectory was computed on the assumption of a chemical propulsion trajectory (a SEP trajectory will be calculated in due course), with the proposed solution of a two impulse transfer – an initial impulse to insert the spacecraft into the first to reach Mars, and a second impulse at aphelion to change the inclination of the orbit to insert above Mars. The total Δv to achieve this insertion is estimated to be approximately 6.55 km s^{-1} (although the figure to insert a spacecraft at the same point by electric propulsion will differ from this), which, by the same calculation as for the GeoStorm mission previously, affords an on-station mission duration of approximately 2.5 years at maximum thrust.

Another point to consider is that the non-Keplerian orbit actually need only be maintained during periods

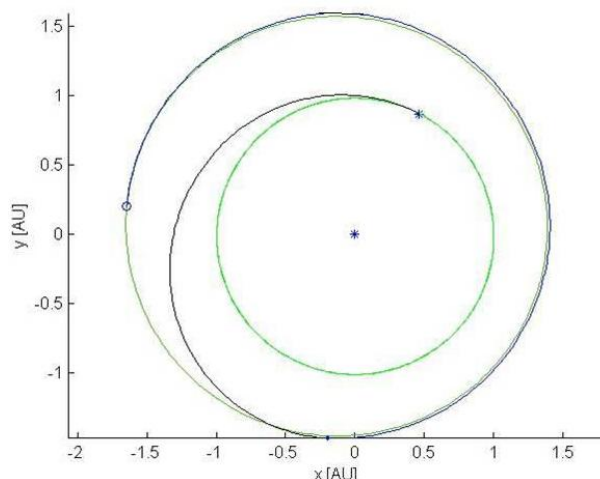


Fig. 21: Earth-Mars interplanetary transfer (grey line) viewed from directly above the Ecliptic plane. The green rings represent the orbits of Earth (inner) and Mars (outer).

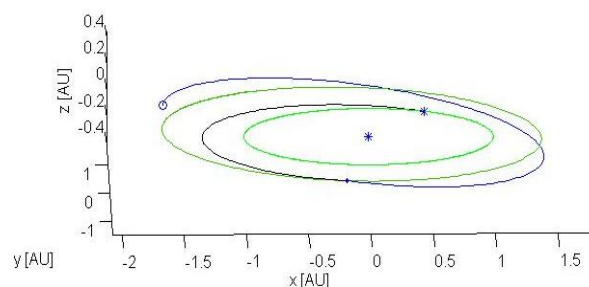


Fig. 22: Earth-Mars interplanetary transfer (grey line) viewed from just above the plane of the Ecliptic. The green rings represent the orbits of Earth (inner) and Mars (outer).

of solar occultation, and hence it may be possible to extend the spacecraft lifetime by only using the thrusters during such periods and allowing the spacecraft to follow a conventional near-Keplerian orbit during other periods. For example, the synodic period of Mars (the temporal interval that it takes for an object to reappear at the same point in relation to two other objects) with respect to Earth and the Sun (and thus the occultation repeat period) is approximately 780 days, whereas the sidereal period (the temporal interval it takes an object to make one full orbit around the sun) is roughly 687 days. Thus one could envisage a mission that would see the SEP spacecraft thrusting to hover above Mars for 93 days to maintain communications whilst Mars is occulted, and then switching off its thrusters and carrying out a Keplerian A orbit for 687 days, naturally returning to the correct point for the next occultation of Mars, where the thruster would be switched back on to occupy the B orbit position again. Thus the craft would only need to thrust for about 90 days in every 2.13-year period (approximately), significantly extending the on-station time as allowed by the thruster propellant reserves.

Of course the alignment of the planets as shown in Figure 14 is of course not the complete picture, as the inclination of the orbit of Mars has to be taken into account as well. Thus a detailed study is required in order to determine exactly where Mars would be in relation to the Ecliptic plane at each occultation: sometimes Mars may be higher or lower in relation to the Earth-Sun line, meaning that the distance the spacecraft would need to hover at above Mars in order to maintain the communications relay would change, and thus the amount of thrust required would also change accordingly. It is also intended that a detailed propulsion failure scenario study be carried out on this mission, which will suggest optimal strategies for recovering a stable orbit in the event of a malfunction.

It may also be possible to use Earth's L_3 point for a similar purpose. However, it is estimated that 300mN would only allow the spacecraft to hover a maximum of approximately 0.05AU above the L_3 point (as shown in Figure 23) compared with the 0.14AU required in order to achieve continuous communications (again assuming a four-degree Solar field-of-view exclusion from Earth).

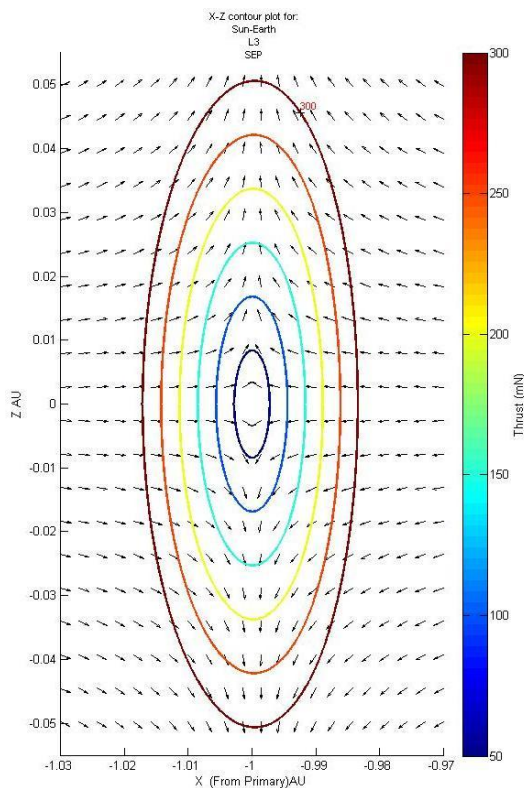


Fig. 23: B orbit zones depicted by equithrust contours around the Earth L_3 point projected onto the plane parallel to the Ecliptic plane, for SEP of thrust values of up to 300mN. The arrows represent the direction of thrust required.

Additionally, it is worth considering the size of antennae needed for communication between the spacecraft, the surface of Earth, and the surface of

Mars. Displacing a spacecraft above Earth's L_3 point would require one large antenna in order to transmit signals across the sizeable distance of 2AU between the Earth and the L_3 hover point and Mars, as well as a medium-sized antenna for transmission across the lesser but still significant 0.52AU between the L_3 point and Mars. The advantage of hovering close to Mars is that whilst one large antenna is still required for communicating between the spacecraft and Earth, 2.52AU away, the second antenna only has to transmit signals across the much shorter distance between the spacecraft and the Martian surface approximately 0.176AU away, or the other (leading or trailing) spacecraft approximately 0.352AU away and thus need not be as large.

In theory, yet another possible way of achieving the same objective would be to consider a Solar hover, i.e. the two-body Sun-centred displaced B orbit directly above the Sun in the plane out of the Ecliptic. As Figure 24 shows, a spacecraft with 300mN of thrust could hover approximately 4.5AU directly above the Sun. In real terms though the distance and extreme difficulty of inserting a spacecraft into such an orbit in the first place would make this impractical for such a purpose – however, it demonstrates the potential that such orbits have.

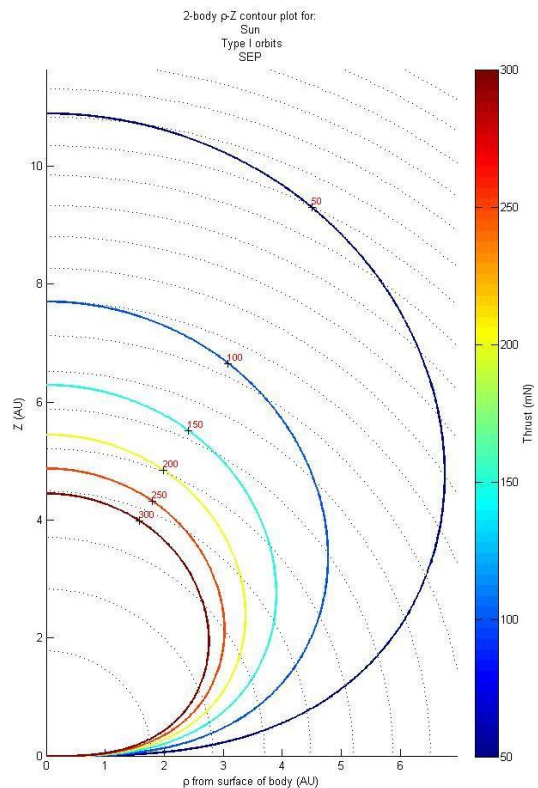


Fig. 24: Equithrust contours depicting the displaced Type I B orbit regions about the Sun. The innermost contour represents a thrust of 300mN (labelled). The dashed lines represent contours of constant orbital period.

VI. SUMMARY

A catalogue of displaced non-Keplerian B orbits for celestial bodies in the Solar system has been systematically created. B orbits could have a diverse range of applications for space physics, exploration and planetary science and thus such a catalogue is important in quickly and efficiently determining which opportunities are enabled by specific spacecraft parameters, such as mass and maximum thrust. B orbits are considered both for the two-body case, where three unique types of orbit exist, parameterised by the orbit period, and for the three-body case, where the orbit period of the spacecraft is fixed to that of the planet it is in the vicinity of. Both solar electric and solar sail propulsion systems are considered, although in the latter case only about the Sun in the two-body case or about a body orbiting the Sun in the three-body case. The SEP case considers either current or near-term technology, such as the QinetiQ T6 thruster. Some example figures are provided and two potential candidate missions utilising B orbits from the catalogue are discussed at length.

Of course, it is important to note that although we consider equithrust surfaces, no propulsion system actually delivers an equal thrust throughout the lifetime of the spacecraft, due to either depletion of reaction-mass or, in the case of solar sailing, the degradation of the optical surface [15]. As such, the propulsion system must be throttled to adjust for either the increasing (for depletion of reaction-mass) or decreasing (for degradation of the optical surface) acceleration vector magnitude.

ACKNOWLEDGEMENTS

This work was funded primarily by ESA Contract Number 22349/09/F/MOS; Study on Gravity Gradient Compensation Using Low Thrust High Isp Motors and by European Research Council Advanced Investigator Grant VISIONSPACE 227571 for C. McInnes.

REFERENCES

- [1] H.M. Dusek, "Optimal station keeping at collinear points", *Progress in Astronautics and Aeronautics*, Vol. 17, pp. 37-44, 1966.
- [2] C.R. McInnes, A.J.C. McDonald, J.F.L. Simmons, E.W. MacDonald, "Solar sail parking in restricted three-body systems", *Journal of Guidance, Dynamics and Control*, Vol. 17, No. 2, pp. 399-406, 1994
- [3] R.L. Forward, "Statite: a spacecraft that does not orbit", *Journal of Spacecraft and Rockets*, Vol. 28, No. 5, pp. 606-611, 1991
- [4] C.R. McInnes, *Solar Sailing: Technology, Dynamics, and Mission Applications*, Praxis Publishing, Chichester, 1999, ISBN 1-85233-102-X.

- [5] S. Baig, C. R. McInnes, "Artificial three-body equilibria for hybrid low-thrust propulsion", *Journal of Guidance, Control and Dynamics*, Vol. 31, No. 6, November-December 2008.
- [6] T.R. Spilker, "Saturn ring observer", *Acta Astronautica*, Vol. 52, p259-265, 2003
- [7] C.R. McInnes, "Dynamics, stability and control of displaced non-Keplerian orbits", *Journal of Guidance, Control, and Dynamics*, Vol. 21, No. 5, September-October 1998
- [8] J. Simo, C.R. McInnes, "Displaced periodic orbits with low-thrust propulsion in the Earth-Moon System", AAS 09-153, 19th AAS/AIAA Space Flight Mechanics Meeting, Savannah, Georgia, February, 2009.
- [9] M. Macdonald, G.W. Hughes, C.R. McInnes, A. Lyngvi, P. Falkner, A. Atzei, "GeoSail: an elegant solar sail demonstration mission", *Journal of Spacecraft and Rockets*, Vol. 44, No. 4, July-August 2007
- [10] M. Leipold, W. Seboldt, S. Ligner, E. Borg, A. Herrmann, A. Pabsch, O. Wagner, J. Bruckner, "Mercury Sun-synchronous polar orbiter with a solar sail", *Acta Astronautica*, Vol. 39, No. 1-4, pp 143-151, 1996
- [11] M. Leipold, E. Borg, S. Ligner, A. Pabsch, R. Sachs, W. Seboldt, "Mercury orbiter with a solar sail spacecraft", *Acta Astronautica*, Vol 35, pp635-644, 1995
- [12] N. Wallace, "Testing of the Qinetiq T6 thruster in support of the ESA BepiColombo Mercury mission", *Proceedings of the 4th International Spacecraft Propulsion Conference (ESA SP-555)*, Chia Laguna, Cagliari, Italy, 2nd-9th June 2004
- [13] J.L. West, "The GeoStorm warning mission: enhanced opportunities based on new technology", 14th AAS/AIAA Spaceflight Mechanics Conference, Paper AAS 04-102, Maui, Hawaii, Feb 8th-12th 2004
- [14] J.L. West, "Solar sail vehicle system design for the GeoStorm warning mission", *Structures, Structural Dynamics and Materials Conference*, Atlanta, USA, April 2000
- [15] B. Dachwald, M. Macdonald, C.R. McInnes, G. Mengali, A.A. Quarta, "Impact of optical degradation on solar sail mission performance", *Journal of Spacecraft and Rockets*, Vol 44., No. 4, pp740-749, 2007